Published in final edited form as:
Magn Reson Med. 2014 July ; 72(1): 26–32. doi:10.1002/mrm.24933.

Two-Dimensional Semi-LASER Correlation Spectroscopy with Well-Maintained Cross Peaks

Meijin Lin[1], **Anand Kumar**[1], and **Shaolin Yang**[1,2,3,*]

[1]Department of Psychiatry, University of Illinois at Chicago, Chicago, Illinois 60612, USA

[2]Department of Radiology, University of Illinois at Chicago, Chicago, Illinois 60612, USA

[3]Department of Bioengineering, University of Illinois at Chicago, Chicago, Illinois 60612, USA

Abstract

Purpose—To demonstrate that the limited bandwidth of the second 90° RF pulse in two-dimensional (2D) localized correlation spectroscopy (L-COSY) induces spatially dependent magnetization transfer that results in attenuated cross-peaks, and to propose a new 2D semi-adiabatically localized COSY sequence to solve this problem.

Methods—A semi-localization by adiabatic selective refocusing (semi-LASER or sLASER) method was incorporated into the COSY sequence with the slice-selective first 90° RF pulse and the non-slice-selective second 90° RF pulse to form a new 2D sLASER localized COSY sequence, named “sLASER-first-COSY”, to solve the problem of spatially dependent magnetization transfer. Experiments were performed to verify the feasibility and advantages of sLASER-first-COSY sequence over a recently reported other sLASER COSY sequence with a slice-selective second 90° RF pulse, named “sLASER-last-COSY”.

Results—Phantom, ex vivo, and in vivo human brain experiments demonstrated that sLASER-first-COSY yielded stronger cross peaks and higher ratios of cross peak volumes to diagonal peak volumes than sLASER-last-COSY.

Conclusion—As COSY relies on the cross peaks to obtain larger dispersion of peaks for quantification, the new sLASER-first-COSY sequence yielding well-maintained cross peaks will facilitate more reliable and accurate quantification of metabolites with coupled spin systems.

Keywords

localization by adiabatic selective refocusing (LASER); two-dimensional (2D); magnetic resonance spectroscopy (MRS); correlation spectroscopy (COSY); cross peak; magnetization transfer; chemical shift displacement error (CSDE)

*Correspondence to: Shaolin Yang, Ph.D., Assistant Professor, Director of Neuro MR Spectroscopy, Departments of Psychiatry and Radiology, University of Illinois at Chicago, 1601 W. Taylor St., Suite 566, Chicago, IL 60612, USA, Phone: 312-413-3818, shaolin@uic.edu.

INTRODUCTION

High-field magnets can increase signal-to-noise ratio (SNR) and chemical shift dispersion in magnetic resonance spectroscopy (MRS) (1–3). However, there are some disadvantages at higher field strengths, such as shorter apparent transverse relaxation time (T_2*) (4–6), longer longitudinal relaxation time (T_1) (5), increased main static field (B_0) inhomogeneity and radiofrequency (RF) field (B_1) inhomogeneity and increased chemical shift displacement error (CSDE) (3). In addition, the available RF power is usually more limited relative to the increased field strengths (2). CSDE is proportional to B_0 and inversely proportional to the bandwidth (BW) of a slice-selective RF pulse (2,7–9). A two-dimensional (2D) localized correlation spectroscopy (L-COSY) sequence includes one slice-selective 180° RF pulse (10), which will contribute to a larger CSDE than a slice-selective 90° RF pulse.

The limited BWs of RF pulses not only cause CSDE but also lead to spatially dependent evolution of J-coupling (11), which results in additional J-refocused artifactual peaks in 2D J-resolved spectroscopy (11–14). Unfortunately, when the BWs of RF pulses are limited, there is a similar issue in L-COSY that one of the coupled spin pair may not undergo the 90° pulses in the voxel selected for its J-coupled partner. Therefore, magnetization transfer will not occur in part of the voxel, which leads to spatially dependent magnetization transfer and thus results in reduced cross peak intensity in L-COSY. As cross peaks contain important information of the metabolites with coupled spin systems, compromised cross peaks will impair the quantification of L-COSY spectra. However, to the best of our knowledge, there is no report of this problem in the literature.

The above issues related to CSDE can be mitigated using adiabatic RF pulses as adiabatic RF pulses offer large BWs and produce a uniform flip angle despite variation in B_1, provided that the B_1 is above a certain threshold. Moreover, they have been applied for localization in MRS (14–18). A basic COSY sequence is composed of two 90° RF pulses. Recently, adiabatic localization were incorporated into COSY sequences: one is LASER, which stands for localization by adiabatic selective refocusing (16) and uses a non-slice-selective excitation pulse followed by three pairs of adiabatic full-passage (AFP) pulses for signal refocusing as well as volume selection, so we call the sequence “LASER-COSY” (1,19), and the other is semi-LASER, which uses two pairs of AFP pulses and the second 90° RF pulse for volume localization (8), so we call the sequence “sLASER-last-COSY”. As LASER-COSY has disadvantages including significantly longer echo time (TE) and higher specific absorption rate (SAR), semi-LASER (2,20,21) seems to be a more appropriate scheme for adiabatically localized COSY in in vivo application.

In this report, we first demonstrated in theory that the cross peaks would be attenuated in L-COSY and sLASER-last-COSY due to spatially dependent magnetization transfer, and we proposed an adiabatically localized COSY sequence with an alternative semi-LASER scheme, which employs the first 90° RF pulse and two pairs of AFP pulses for volume localization and a non-slice-selective second 90° pulse for magnetization transfer, to solve this problem. Accordingly we call the proposed sequence “sLASER-first-COSY”. Experiments on phantoms, fresh pig brain tissue (ex vivo) and human brain (in vivo) were

performed to verify the feasibility and demonstrate the advantages of sLASER-first-COSY over sLASER-last-COSY.

METHODS

Pulse Sequences

Figure 1 shows two versions of sLASER COSY sequences: sLASER-first-COSY (Fig. 1a) and sLASER-last-COSY (Fig. 1b). Both sequences contain two pairs of AFP pulses for slice selections in two orthogonal planes. In sLASER-last-COSY sequence (8), the mixing pulse (i.e., the second 90° pulse) is used for selection of the third orthogonal plane. In contrast, in sLASER-first-COSY sequence the excitation pulse (i.e., the first 90° pulse) is used for selection of the third orthogonal plane while the second 90° pulse is only used as the mixing pulse for COSY but not for slice selection. In both sequences, crusher gradients and 8-step phase cycling are applied for suppressing unwanted free induction decays (FIDs). The more steps of phase cycling are applied, the less contamination comes from unwanted coherence transfer pathways, if motion is negligible during the scan. The phases of the first 90° pulse, four AFP pulses, the second 90° pulse, and the receiver for the 8-step phase cycling are (x, y, −x, −y, x, y, −x, −y), (x, x, x, x, −x, −x, −x, −x), (x, −x, x, −x, x, −x, x, −x), and (x, −y, −x, y, x, −y, −x, y), respectively. The total scan duration is less than 14 minutes.

In both sequences the spoiler gradients around the second 90° RF pulses have an area of 44 mT/m·ms, a default setting in the Philips product sequence. However, the spoiler gradients for AFP pulses can be relatively small, because the profile of a pair of AFP pulses is quite sharp, and the residual refocusing outside the pass band is negligible (16,21). A series of gradient-time integral values of spoiler gradients were tested to find the optimal design for suppressing artifacts in the in vivo experiments. For each pair of AFP pulses, the spoiler gradients were 10 mT/m with a duration of 0.31 ms (155 μs ramp-up/down times without top) around the first AFP pulse and 8 mT/m and 0.31 ms (155 μs ramp-up/down times without top) around the second AFP pulse for the phantom and ex vivo experiments, while the duration of spoiler gradients was 1.81 ms with 1.5 ms of top for the in vivo experiments.

Theory

In conventional localized COSY, if a pair of coupled spins have a large chemical shift difference, one spin may not undergo the second 90° RF pulse in a part of the slice selected for its J-coupled partner due to a finite BW of the slice-selective second 90° RF pulse. As a result, the magnetization in that specific part of slice cannot be transferred between coupled spins and the cross peaks cannot be formed. This problem can be solved if the second 90° pulse is not used for slice selection.

Now we investigate the effect of scalar coupling on signal formation of localized COSY ignoring relaxation, diffusion, etc. We consider a homonuclear J-coupled I_1I_2 spin-1/2 system with a coupling constant J. In part of the plane excited by a slice-selective pulse for spin I_1, spin I_2 does not experience the pulse due to the chemical shift displacement between spins I_1 and I_2 (13). The mixing RF pulse is critical in forming cross peaks, so the performance of the second 90° pulse on spin I_2 will be considered. If the second 90° RF

pulse is used for slice selection, we can decompose the voxel into two distinct subvoxels: subvoxel 1 (spin I_2 undergoes the second 90° RF pulse) and subvoxel 2 (spin I_2 does not undergo the second 90° pulse). The raising/lowering operators I^+/I^-, transitions up/down between energy levels, are used in the following deduction. Assuming an equilibrium condition of spin I is I_z, after the first 90° RF pulse with a phase along the direction x, I_{1z} transforms into $(-i/2)I_1^-$ in the L-COSY sequence. After the 180° RF pulse in L-COSY sequence, the above spin term evolves as $(-i/2)I_1^+$. During the evolution time t_1, the spin term evolves under the chemical shift and J-coupling as

$$-\frac{i}{2}I_1{}^+\cos(\pi Jt_1)e^{-i\Omega_1 t_1}-\frac{1}{2}\cdot 2I_1{}^+I_{2z}\sin(\pi Jt_1)e^{-\Omega_1 t_1}, \quad (1)$$

where the Ω_i is the frequency offset of spin i (i = 1, 2) in the rotating frame. In subvoxel 1 when the second 90° RF pulse is used for slice selection or in the whole voxel when the second 90° RF pulse is not used for slice selection, the second 90° RF pulse is effective on both spins, so the above terms will be converted to

$$-\frac{i}{4}I_1{}^-\cos(\pi Jt_1)e^{-i\Omega_1 t_1}-\frac{1}{4}\cdot 2I_{1z}I_2{}^-\sin(\pi Jt_1)e^{-i\Omega_1 t_1}, \quad (2)$$

where the second term is magnetization transfer from spin I_1 to spin I_2 through J-coupling. Finally, during the evolution time t_2, the detectable spin terms evolve under the chemical shift and J-coupling as

$$\begin{aligned}&-\tfrac{i}{4}I_1{}^-\cos(\pi Jt_1)e^{-i\Omega_1 t_1}\cos(\pi Jt_2)e^{i\Omega_1 t_2}-\tfrac{i}{4}I_2{}^-\sin(\pi Jt_2)e^{i\Omega_1 t_1}\sin(\pi Jt_2)e^{i\Omega_2 t_2}\\ =&-\tfrac{i}{4}I_1{}^-\cos(\pi Jt_1)\cos(\pi Jt_2)e^{-i\Omega_1(t_1-t_2)}-\tfrac{i}{4}I_2{}^-\sin(\pi Jt_1)e^{-i\Omega_1 t_1}\sin(\pi Jt_2)e^{i\Omega_2 t_2},\end{aligned} \quad (3)$$

where the first term forms diagonal peaks and the second term cross peaks. However, when the mixing RF pulse is used for slice selection, the second 90° RF pulse is effective only on spin I_1 in subvoxel 2, so the terms in the Eq. (2) will be converted to

$$-\frac{i}{4}I_1{}^-\cos(\pi Jt_1)e^{-i\Omega_1 t_1}-\frac{i}{4}\cdot 2I_1{}^-I_{2z}\sin(\pi Jt_1)e^{-i\Omega_1 t_1}, \quad (4)$$

where there is no magnetization transfer in the second term. During the evolution time t_2, the detectable spin terms evolve under the chemical shift and J-coupling as

$$\begin{aligned}&-\tfrac{i}{4}I_1{}^-\cos(\pi Jt_1)e^{-i\Omega_1 t_1}\cos(\pi Jt_2)e^{i\Omega_1 t_2}-\tfrac{i}{4}I_1{}^-\sin(\pi Jt_1)e^{-i\Omega_1 t_1}\sin(\pi Jt_2)e^{i\Omega_1 t_2}\\ &=-\tfrac{i}{4}I_1{}^-\cos[\pi J(t_1-t_2)]e^{-i\Omega_1(t_1-t_2)},\end{aligned} \quad (5)$$

which includes only diagonal peaks but no cross peaks. As consequence, the cross peaks in L-COSY will be reduced. The intensity of cross peaks will be reduced by a factor of $1-\frac{\Delta\delta\cdot \mathrm{f}_0}{\mathrm{BW}}$, where f_0 is the resonance frequency, $\Delta\delta$ is the chemical shift difference (in ppm)

of the spins I_1 and I_2, BW is the bandwidth (in Hz) of the slice-selective second 90° pulse (11). It can be concluded that the second 90° RF pulse with a limited BW reduces the intensities of cross peaks, which will impair spectral quantification if this factor is not considered. Take lactate as an example, the chemical shift difference $\Delta\delta$ is 2.8 ppm, which will result in 18% loss of cross peaks, if assuming f_0 = 127.74 MHz at 3 Tesla (T) and BW = 2000 Hz. The same issue will appear in sLASER-last-COSY as the second 90° RF pulse is used for slice selection too. However, the peak intensities also depend on pulse profiles, the apparent transverse relaxation time T_2*, and the duration from excitation to starting of data acquisition in the sequence. It was reported that due to better pulse profiles and possibly longer T_2*, improved SNR was observed using adiabatic sequences compared with a nonadiabatic regular sequence (8,14).

Therefore, if the mixing pulse is not used for slice selection, magnetization will be fully transferred from I_1 to I_2 and the intensities of cross peaks can be well maintained in sLASER-first-COSY. In theory, for a homonuclear J-coupled I_1I_2 spin-1/2 system the cross peak volume should be equal to the diagonal peak volume and the proposed sLASER-first-COSY sequence can completely recover the cross peak. However, imperfect pulse profiles can still contribute to losses in the cross peaks to some extent.

Phantom, Pig Brain Tissue, Human Subjects, and Instrumental Setup

All experiments were performed on a Philips Achieva 3T whole-body scanner (Philips Medical Systems, Best, the Netherlands), operating at the proton resonance frequency f_0 = 127.74 MHz. The body coil was used for transmission and a Philips SENSE-Head-8 coil for reception. The clinically available maximum B_1 is 13.5 μT.

The GE MRS Braino phantom (General Electric Medical Systems, Milwaukee, WI) contained the following metabolites and chemicals: 12.5 mM *N*-acetyl-aspartate (NAA), 10 mM creatine hydrate (Cr), 3 mM choline chloride (Cho), 7.5 mM *myo*-inositol (mI), 12.5 mM glutamate (Glu), and 5 mM lactate (Lac) (10,22). Experiments on the GE MRS Braino phantom, fresh pig brain tissue, and human subjects were performed to verify the feasibility and compare sLASER-first-COSY with sLASER-last-COSY. Written informed consent was obtained from the human subjects and the study was approved by the local IRB.

Experiments on GE MRS Braino Phantom, Pig Brain Tissue, and Human Brain

The parameters of two sLASER COSY sequences in the experiments on GE MRS Braino phantom and pig brain tissue were as follows: voxel size = 30×30×30 mm^3 for GE MRS Braino phantom and 18×18×18 mm^3 for pig brain tissue, number of signal averages (NSA) = 8, repetition time (TR) = 1600 ms, minimum time from excitation to starting of data acquisition = 34 ms and 37 ms for sLASER-first-COSY and sLASER-last-COSY, respectively, 64 t_1 steps with an incremental size Δt_1 = 0.8 ms, 1024 × 64 points were acquired with spectral widths of 2000 Hz × 1250 Hz in the F2 × F1 dimensions, scan duration = 13 mins and 39 s.

For the in vivo experiments on human brain, a 30×30×30 mm^3 voxel was placed aligned with the parieto-occipital junction of two healthy volunteers. The durations of all spoiler

gradients around the AFP pulses were 1.81 ms and the minimum time from excitation to starting of acquisition were 48 ms and 50 ms in sLASER-first-COSY and sLASER-last-COSY, respectively. The other parameters were the same as those used in the experiments on the GE MRS Braino phantom and pig brain tissue.

Spectral Data Processing and Analysis

The 2D MRS data were processed using the Felix software (Accelrys Inc. San Diego, CA, USA). The datasets were zero-filled from 1024 to 2048 points in F2 and from 64 to 256 points in F1. A solvent suppression with a sinebell window function of 20 Hz was applied. A size of 2048 points and a phase of 40° were applied to F2. A size of 256 points and a phase of 40° were applied to F1. A custom-made Matlab program was used for quantification of peak volumes using the method of intensity integration over peak area.

RESULTS

The sLASER-first-COSY and sLASER-last-COSY spectra acquired from the GE MRS Braino phantom are shown in Fig. 2a and b, respectively. Table 1 shows the quantification results of these two spectra, in which all the cross peaks in sLASER-first-COSY are stronger than those in sLASER-last-COSY both in absolute intensity as well as the ratio to diagonal peak.

The sLASER-first-COSY and sLASER-last-COSY spectra of fresh pig brain tissue are shown in Fig. 2c and d. The cross peak volumes and associated peak volume ratios are shown in Table 2. The quantification results show that all the cross peaks in sLASER-first-COSY are stronger than those in sLASER-last-COSY, and all the ratios of the cross peak volumes to the associated diagonal peak volumes are also larger in sLASER-first-COSY.

The sLASER-first-COSY and sLASER-last-COSY spectra acquired from a voxel encompassing the parieto-occipital junction of a healthy volunteer are shown in Fig. 2e and f. The quantification results of the spectra from two healthy volunteers (including the one in Fig. 2e and f) are shown in Table 3. Nearly all the cross peak volumes (shown in Fig. 2e and f) and the ratios of the cross peak volumes to associated diagonal peak volumes (shown in Table 3) are larger in sLASER-first-COSY than those in sLASER-last-COSY.

DISCUSSION AND CONCLUSIONS

The experiments were performed on GE Braino phantom, fresh pig brain tissue, and human brains in vivo. The experiment results showed that not only the cross peak volumes but also the ratios of cross peak volumes to associated diagonal peak volumes were larger in sLASER-first-COSY than in sLASER-last-COSY, which proves that cross peaks can be better maintained in sLASER-first-COSY than in sLASER-last-COSY.

Compared to conventional L-COSY (10), sLASER-first-COSY yielded most of peaks with higher SNR and sLASER-last-COSY yielded some peaks with higher SNR in the spectra of GE MRS Braino phantom and pig brain tissue (L-COSY spectra not shown), though the durations from the excitation to the starting of data acquisition in sLASER-first-COSY and sLASER-last-COSY were 10 and 13 ms longer than that in L-COSY, respectively. This is

because a pair of AFP pulses can provide better pulse profiles than a nonadiabatic regular pulse (8,14).

Compared with the ratios of cross peak volumes to diagonal peak volumes in the spectra of GE MRS Braino phantom in Table 1, the ratios are smaller in the spectra of pig brain tissue and human brain in Tables 2 and 3. This is because there are more peaks from other metabolites overlapping with the diagonal peaks in the spectra of pig brain tissue and human brain than those in the spectra of GE MRS Braino phantom (containing only 6 metabolites, while about 20 metabolites detectable in the pig brain tissue and human brain). Taking Lac as an example, the Lac diagonal peaks overlap with the lipids (Lip)/macromolecules (MM) diagonal peaks at 1.31 ppm in the spectra of pig brain tissue and human brain. In contrast, there are no Lip/MM in the phantom and therefore no Lip/MM diagonal peaks overlapping with the Lac diagonal peaks in the phantom spectra. Because there are no overlap between the Lip/MM cross peaks and the Lac cross peaks at (4.10 ppm, 1.31 ppm) in COSY spectra, the peak ratios of Lac in the spectra of pig brain tissue are smaller than those in the spectra of GE MRS Braino phantom (Lac peak not shown clearly in human brain spectra because of very low concentration in normal brain tissue). Peak volumes estimated by the method of intensity integration over peak area can be biased due to peak overlap. However, the biased values caused by cross peaks overlapping cross peaks or diagonal peaks overlapping with diagonal peaks can still be used to qualitatively compare the performance of the two sLASER COSY sequences. To mitigate the above issues, it is better to implement 2D fitting of the COSY spectra with the 2D version of “basis functions” or “modal spectra” (23), similar with the LCModel analysis of 1D spectra (24).

The striping artifacts, i.e., ridges of noises running parallel to the F1 and F2 axis (but mainly along the F1 dimension), are described as t_1 and t_2 noise, respectively (25). The t_1 and t_2 noises are evident wherever there are strong peaks in the 2D spectrum. The intensities of both artifacts are proportional to the peak amplitude (25). Because at the same concentrations the metabolite resonances are always weaker in ex vivo and in vivo spectra than in phantom spectra due to the T_2 relaxation effects, the striping artifacts are more evident in phantom spectra. This is why the t_1 noises are clearly presented in the phantom spectra (Fig. 2a and b) but less evident in the spectra of pig brain tissue (Fig. 2c and d) and human brain (Fig. 2e and f).

In conclusion, this study demonstrated that cross peaks are attenuated in localized COSY spectra if the second 90° RF pulse (i.e., the mixing pulse) is used for slice selection but having a limited bandwidth, for example, in L-COSY and sLASER-last-COSY. An improved version of sLASER COSY sequence, called sLASER-first-COSY, was proposed to prevent the cross peaks from attenuation due to spatially dependent magnetization transfer. Experiments on phantom, fresh pig brain tissue, and human brain in vivo demonstrated that sLASER-first-COSY yielded well-maintained cross-peaks compared with sLASER-last-COSY. As COSY relies on the cross peaks to obtain larger dispersion of peaks for quantification, sLASER-first-COSY yielding well-maintained cross peaks will facilitate more reliable and accurate quantification of metabolites with coupled spin systems than sLASER-last-COSY. Although LASER-COSY sequence (1) can also fully transfer magnetization, the duration from excitation to starting of data acquisition is significantly

longer than sLASER-first-COSY and the overall SNR will be lower. Therefore, sLASER-first-COSY will be a more suitable localized COSY method for in vivo application.

Acknowledgments

Grant sponsor: NIH; grant numbers: R01 MH63764 and R01 MH73989.

References

1. Andronesi OC, Ramadan S, Mountford CE, Sorensen AG. Low-power adiabatic sequences for in vivo localized two-dimensional chemical shift correlated MR spectroscopy. Magn Reson Med. 2010; 64:1542–1556. [PubMed: 20890988]
2. Boer VO, van Lier ALHM, Hoogduin JM, Wijnen JP, Luijten PR, Klomp DWJ. 7-T ^{1}H MRS with adiabatic refocusing at short TE using radiofrequency focusing with a dual-channel volume transmit coil. NMR Biomed. 2011; 24:1038–1046. [PubMed: 21294206]
3. Kinchesh P, Ordidge RJ. Spin-echo MRS in humans at high field: LASER localisation using FOCI pulses. J Magn Reson B. 2005; 175:30–43.
4. Mason GF, Pohost GM, Hetherington HP. Numerically Optimized Experiment Design for Measurement of Grey/White Matter Metabolite T_2 in High-Resolution Spectroscopic Images of Brain. J Magn Reson B. 1995; 107:68–73. [PubMed: 7743075]
5. Posse S, Cuenod CA, Risinger R, Lebihan D, Balaban RS. Anomalous transverse relaxation in ^{1}H spectroscopy in human brain at 4 Tesla. Magn Reson Med. 1995; 33:246–252. [PubMed: 7707916]
6. Michaeli S, Garwood M, Zhu XH, DelaBarre L, Andersen P, Adriany G, Merkle H, Ugurbil K, Chen W. Proton T_2 relaxation study of water, N-acetylaspartate, and creatine in human brain using Hahn and Carr-Purcell spin echoes at 4 T and 7 T. Magn Reson Med. 2002; 47:629–633. [PubMed: 11948722]
7. Andronesi OC, Ramadan S, Ratai EM, Jennings D, Mountford CE, Sorensen AG. Spectroscopic imaging with improved gradient modulated constant adiabaticity pulses on high-field clinical scanners. J Magn Reson. 2010; 203:283–293. [PubMed: 20163975]
8. Ramadan S, Mountford CE. Adiabatic localized correlation spectroscopy (AL-COSY): application in muscle and brain. J Magn Reson Imaging. 2011; 33:1447–1455. [PubMed: 21591015]
9. de Graaf, RA. *In vivo* NMR spectroscopy - Principles and techniques. Chichester, UK: John Wiley; 1998.
10. Thomas MA, Yue K, Binesh N, Davanzo P, Kumar A, Siegel B, Frye M, Curran J, Lufkin R, Martin P, Guze B. Localized two-dimensional shift correlated MR spectroscopy of human brain. Magn Reson Med. 2001; 46:58–67. [PubMed: 11443711]
11. Edden RAE, Barker PB. If J doesn't evolve, it won't J-resolve: J-PRESS with bandwidth-limited refocusing pulses. Magn Reson Med. 2011; 65:1509–1514. [PubMed: 21590799]
12. Thompson RB, Allen PS. Sources of variability in the response of coupled spins to the PRESS sequence and their potential impact on metabolite quantification. Magn Reson Med. 1999; 41:1162–1169. [PubMed: 10371448]
13. Yablonskiy DA, Neil JJ, Raichle ME, Ackerman JJH. Homonuclear J coupling effects in volume localized NMR spectroscopy: Pitfalls and solutions. Magn Reson Med. 1998; 39:169–178. [PubMed: 9469698]
14. Lin MJ, Kumar A, Yang SL. Two-dimensional J-resolved LASER and semi-LASER spectroscopy of human brain. Magn Reson Med. 201310.1002/mrm.24732
15. de Graaf RA, Luo Y, Terpstra M, Merkle H, Garwood M. A new localization method using an adiabatic pulse, BIR-4. J Magn Reson B. 1995; 106:245–252. [PubMed: 7719624]
16. Garwood M, DelaBarre L. The return of the frequency sweep: Designing adiabatic pulses for contemporary NMR. J Magn Reson. 2001; 153:155–177. [PubMed: 11740891]
17. Sacolick LI, Rothman DL, de Graaf RA. Adiabatic refocusing pulses for volume selection in magnetic resonance spectroscopic imaging. Magn Reson Med. 2007; 57:548–553. [PubMed: 17326179]

18. Tannus A, Garwood M. Adiabatic pulses. NMR Biomed. 1997; 10:423–434. [PubMed: 9542739]
19. Andronesi OC, Kim GS, Gerstner E, Batchelor T, Tzika AA, Fantin VR, Vander Heiden MG, Sorensen AG. Detection of 2-hydroxyglutarate in *IDH*-mutated glioma patients by in vivo spectral-editing and 2D correlation magnetic resonance spectroscopy. Sci Transl Med. 2012; 4:116ra4.
20. Scheenen TWJ, Heerschap A, Klomp DWJ. Towards ^{1}H-MRSI of the human brain at 7T with slice-selective adiabatic refocusing pulses. Magn Reson Mat Phys Biol Med. 2008; 21:95–101.
21. Scheenen TWJ, Klomp DWJ, Wijnen JP, Heerschap A. Short echo time ^{1}H-MRSI of the human brain at 3T with minimal chemical shift displacement errors using adiabatic refocusing pulses. Magn Reson Med. 2008; 59:1–6. [PubMed: 17969076]
22. Schirmer T, Auer DP. On the reliability of quantitative clinical magnetic resonance spectroscopy of the human brain. NMR Biomed. 2000; 13:28–36. [PubMed: 10668051]
23. Schulte RF, Boesiger P. ProFit: two-dimensional prior-knowledge fitting of J-resolved spectra. NMR Biomed. 2006; 19(2):255–263. [PubMed: 16541464]
24. Provencher SW. Estimation of metabolite concentrations from localized in-vivo proton NMR-spectra. Magn Reson Med. 1993; 30:672–679. [PubMed: 8139448]
25. Mehlkopf AF, Korbee D, Tiggelman TA, Freeman R. Sources of t_1 noise in two-dimensional NMR. J Magn Reson. 1984; 58:315–323.

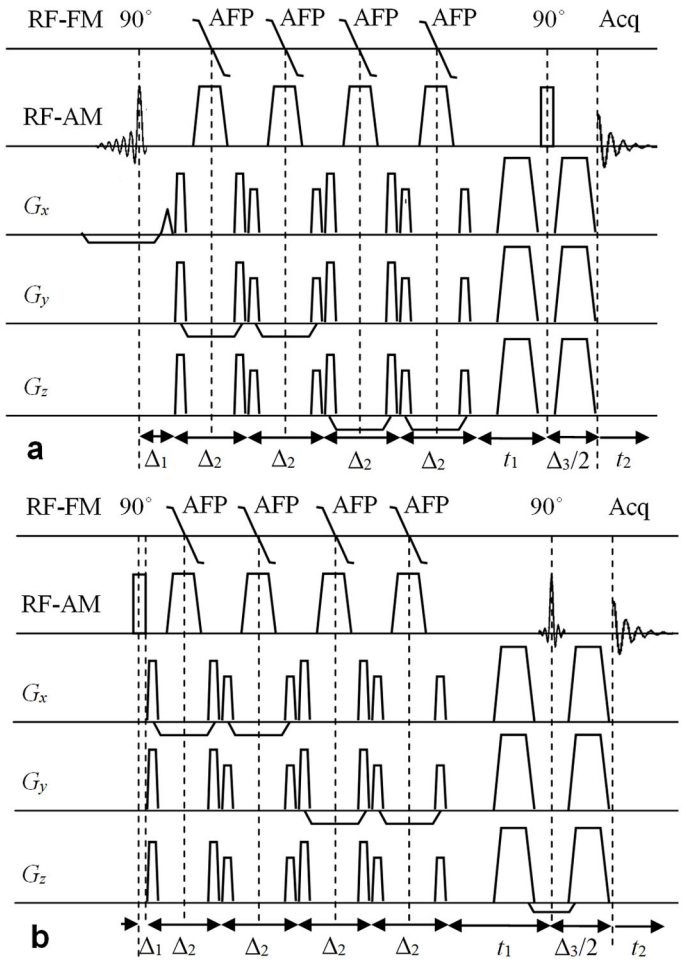

Fig. 1.

Two versions of sLASER COSY sequences: (a) sLASER-first-COSY and (b) sLASER-last-COSY. RF-AM shows the amplitude modulation profiles of the pulses, RF-FM the frequency modulation profiles. Δ_1 is the interval between the excitation RF pulse and the beginning of the first AFP spoiler gradient. Δ_2 is the interval between a pair of AFP spoiler gradients, including the AFP pulse. Δ_3 is the interval between the last pair of spoiler gradients, including the second 90° RF pulse.

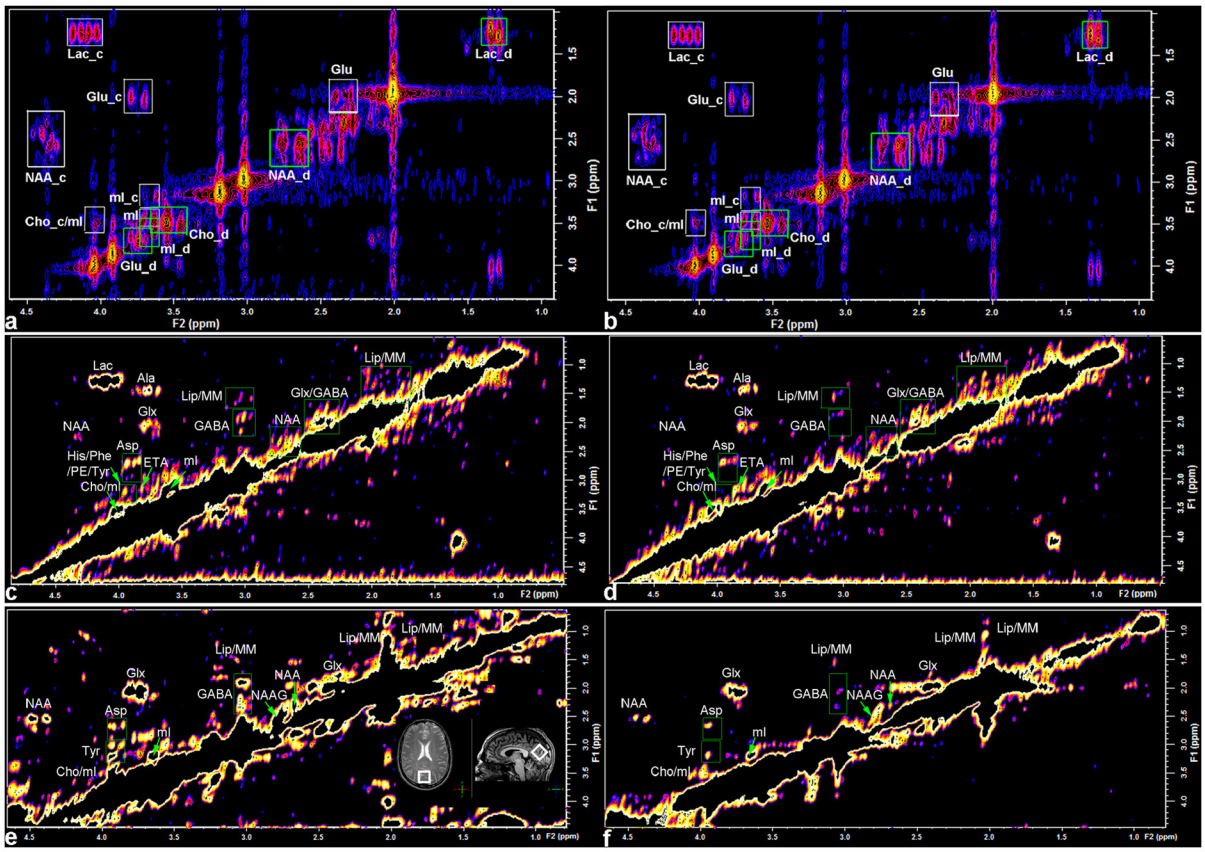

Fig. 2.

Spectra of sLASER-first-COSY (a, c, and e) and sLASER-last-COSY (b, d, and f) acquired from GE MRS Braino phantom (top row), fresh pig brain tissue (middle row), and parieto-occipital junction of a healthy volunteer (see the inset) (bottom row). All cross peaks are stronger in sLASER-first-COSY than sLASER-last-COSY. Two versions of spectra in each row are displayed with the same scale. In the phantom spectra (top row), _c after names of metabolites indicates cross peaks and _d indicates diagonal peaks. Abbreviations used: Lip = lipid; MM = macromolecule; Glu = glutamate; Glx = glutamate plus glutamine; GABA = γ-aminobutyric acid; NAA = *N*-acetyl-aspartate; NAAG = *N*-acetylaspartylglutamate; mI = *myo*-inositol; Ala = alanine; Asp = aspartate; ETA = Ethanolamine; Lac = lactate; His = histidine; Phe = Phenylalanine; PE = phosphorylethanolamine; Tyr = tyrosine; Cho = choline.

Table 1

Cross peak volumes and ratios of cross peak volumes to associated diagonal peak volumes in sLASER-first-COSY and sLASER-last-COSY spectra of GE MRS Braino phantom in Fig. 2a and b.

Cross peak/Diagonal peak	sLASER-first-COSY		sLASER-last-COSY	
	cross peak volume	ratio	cross peak volume	ratio
Lac(4.10,1.31)/Lac_d(1.31)	305	0.92	196	0.66
NAA(4.38,2.58)/NAA_d(2.58)	650	0.56	372	0.30
Cho(4.05,3.50)/Cho_d(3.50)	360	0.56	183	0.29
Glu(3.74,2.08)/Glu_d(3.74)	336	0.69	199	0.45
Glu(2.34,2.08)/Glu_d(2.34)	1113	1.22	1002	1.17
mI(3.61,3.52)/mI_d(3.61)	1117	1.10	987	1.02
mI(3.61,3.27)/mI_d(3.61)	741	0.73	557	0.58

For cross peaks, peak locations are indicated as peak name(F2, F1) with two values in ppm in F2 and F1 axes, respectively; for diagonal peaks, peak locations are indicated as peak name_d(F2) with only one value in ppm for both F2 and F1 axes (same in all other tables).

Table 2

Cross peak volumes and ratios of cross peak volumes to associated diagonal peak volumes in sLASER-first-COSY and sLASER-last-COSY spectra of fresh pig brain tissue in Fig. 2c and d.

Cross peak/Diagonal peak	sLASER-first-COSY		sLASER-last-COSY	
	cross peak volume	ratio	cross peak volume	ratio
Lac(4.10,1.31)/Lac_d(1.31)	50	0.43	44	0.37
Ala(3.77,1.47)/Ala_d(1.47)	25	0.44	21	0.33
Asp(3.89,2.73)/Asp_d(2.73)	45	0.30	30	0.20
NAA(4.38,2.58)/NAA_d(2.58)	34	0.20	21	0.12
Cho(4.05,3.50)/Cho_d(3.50)	39	0.19	30	0.17
Glu(3.74,2.08)/Glu_d(3.74)	34	0.17	26	0.15
mI(3.61,3.27)/mI_d(3.61)	164	0.52	134	0.50
GABA(3.01,1.89)/GABA_d(1.89)	64	0.15	60	0.14

Table 3

Ratios of cross peak volumes to associated diagonal peak volumes in sLASER-first-COSY and sLASER-last-COSY spectra from a voxel encompassing parieto-occipital junction of two healthy volunteers. Spectra from Subject 1 are shown in Fig. 2e and f. Ratios in Subject 1 and 2 are very similar.

Ratio	sLASER-first-COSY		sLASER-last-COSY	
	Subject 1	Subject 2	Subject 1	Subject 2
Asp(3.89,2.73)/Asp_d(2.73)	0.23	0.23	0.15	0.16
NAA(4.38,2.58)/NAA_d(2.58)	0.29	0.24	0.25	0.20
Cho(4.05,3.50)/Cho_d(3.50)	0.26	0.26	0.23	0.19
Glu(3.74,2.08)/Glu_d(3.74)	0.30	0.34	0.27	0.29
mI(3.61,3.27)/mI_d(3.61)	0.44	0.42	0.43	0.46
GABA(3.01,1.89)/GABA_d(1.89)	0.10	0.11	0.10	0.09